



## INVESTIGATION OF PERFORMANCE OF SOLAR POWERED WATER GENERATOR

 S. Sami

Research Center for Renewable Energy Catholic University of Cuenca,  
Cuenca Ecuador, TransPacific Energy, Inc. Las Vegas, NV, USA.  
Email: [dr.ssami@transpacenergy.com](mailto:dr.ssami@transpacenergy.com) Tel: 7606598460



### ABSTRACT

#### Article History

Received: 29 November 2019

Revised: 8 January 2020

Accepted: 12 February 2020

Published: 10 March 2020

#### Keywords

Solar PV

Modeling

Dehumidification

conservation equations

Validation with experimental work.

The objective of this study is to investigate and analyze the performance of solar water generator that produces potable clean water after a dehumidification process. The numerical model presented in this study was established after the conservation of mass and energy equations of the different subsystems of the solar powered water generator. The model was numerically solved under different conditions such as solar radiation, air humidity, air temperature and different air stream flows. The ratings of the dehumidifier are higher of at higher water production rate at lower solar radiation. The results showed that the lower the humidity ratio the higher the evaporator thermal capacity and that the higher the rate of water production the higher the evaporator thermal capacity as well as higher water production was associated with higher air flow and compressor power consumption. In addition, it was concluded that the lower the ambient temperature the higher the hybrid system efficiency and also the hybrid system efficiency increased at lower ambient temperature and higher water production rate. Finally, the predicted results were in fair agreement with experimental data published in the literature.

**Contribution/Originality:** This study contributes to the existing literature by presenting a comprehensive numerical model to analyze the parameters that impact the performance of generating water from ambient air. Finally, this mathematical model can be used as design tool for solar power generators at different capacities to produce clean water.

## 1. INTRODUCTION

The drinking water shortage and the scarcity of electrical energy in the remote areas are the most important issue in many underdeveloped countries. The United Nations has predicted that 48 countries will experience water stress or scarcity by 2025 (Jury & Vaux Jr, 2007). Four billion people in the world face at least one month of water scarcity every year (Mekonnen & Hoekstra, 2016). The water crisis has or will soon turn into food crisis in many areas of the world (Abdullahi, Ayegba, & Adejoh, 2017; Bagheri, 2018; Suryaningsih & Nurhilal, 2016).

Solar energy has many useful applications, particularly, for generation of electricity for rural areas. Solar energy has significant advantages including environmentally friendly, noise and pollution free, also considered as renewable energy and maintenance is not an issue in remote areas (Abdullahi et al., 2017). This reference also reported that the solar radiation is affected by both mean air temperature and relative humidity.

Suryaningsih and Nurhilal (2016) developed an Atmospheric Water Generator (AWG) prototype based on Thermo-electric cooler (TEC) suitable renewable energy resource. Computational Fluid Dynamics (CFD) was

utilized to optimize the design process. Some parameters such as temperature, moisture content, air flow, pressure, form of air flow channel and the water productivity per unit input of energy were studied. The results were presented as and compared with other conventional commercial products.

Several studies have been reported in the literature that focused on the process and functionality of ambient water harvesting (AWH) systems (Bergmair, Metz, De Lange, & Van Steenhoven, 2014; Habeebullah, 2009; Scrivani & Bardi, 2008; Sharan, Beysens, & Milimouk-Melnytchouk, 2007). But, most of these studies have focused the viability of the process, rather than the process itself, especially near tropical and coastal areas where temperature and humidity levels are typically high (Bergmair et al., 2014; Beysens, Milimouk, Nikolayev, Muselli, & Marcillat, 2003; Ekad, Pawar, Yeole, Taksale, & Gajjar, 2018; Fahmy, Nafeh, Ahamed, & Farghally, 2010; Firmanda, Ihtsham, & Shiraz Aris, 2011; Hellström, 1969; Milani, Qadir, Vassallo, Chiesa, & Abbas, 2014; Nikolayev et al., 1996; NIST, 2013; Sami & Campoverde, 2018; VanWynen & Sonntag, 1985) (<https://physics.stackexchange.com/2019>, 2019; <https://www.epa.gov/water-research/atmospheric-water-generation-research>, 2019; <https://www.watergen.com/technology/>, 2020).

Solar-powered Atmospheric Water Generator that employs dehumidification/condensing technology, that extracts water present in the air in the form of vapor by applying Peltier effect of Thermo-Electric Cooling was discussed in reference (VanWynen & Sonntag, 1985). The system consists of cooling elements, heat exchanger and air circulation unit. A Solar PV unit with adequate current output powered the cooling elements through a controlling circuit. Experiments conducted by the authors, have shown that Solar-energy based AWG are able to produce around 24L/day. Also, this paper presented an overview of the AWG different technologies and, in particular Solar based AWG using Peltier effect.

EPA published in 2019, a study presented in reference (<https://www.epa.gov/water-research/atmospheric-water-generation-research>, 2019) to evaluate the microbial quality of untreated condensate and produced treated water from a Watergen GEN-350 unit (<https://www.watergen.com/technology/>, 2020) during three months of continuous operation. The study concluded that in the absence of disinfection substances/system, there can be microorganisms as determined by HPC. Also, the study pointed out that these microorganisms may not represent a direct human health risk, but positive HPC results suggest favorable conditions for microbial growth. Furthermore, the study of the EPA reported that the primary microorganisms of human health concern are opportunistic pathogens that can grow in drinking water infrastructure, such as *Legionella spp.* and *Mycobacterium spp.*

A recent numerical modelling has been presented by reference (Kabeel, Abdulaziz, & El-Said, 2016) to provide accurate results with cost and time saving. In this paper the fluid flow region was assumed. In the proposed system, four parameters were studied; the pressure drop over the flow bath, the water productivity per square meter, the goal parameter and the influence of ambient temperature as well as humidity. The ambient conditions were considered as the design parameters.

A paper on the feasibility study on the use of an atmospheric water generator (AWG) to capture fresh water in the region of Matehuala, SLP was reported by reference (Julio et al., 2019). This region was found to have the appropriate environmental conditions to use AWGs, with an annual average relative humidity (RH).

of approximately 60%. Moreover, a mathematical model was presented of a dehumidifier, water harvesting can be evaluated under the region's prevailing climatic conditions.

Refence (Liu et al., 2017) studied a portable water generator with two thermoelectric coolers (TECs) that was designed and experimentally investigated in this study. The study included different inlet air relative humidity (RH) and air flow rates were investigated to obtain their impacts on the amount of generated water and condensation rate. This study had a guiding role in designing and optimizing a high-efficient portable water generator.

As pointed out in reference (<https://www.marketwatch.com/press-release/at-239-cagr-atmospheric-water-generator-awg-market-set-to-generate-revenue-of-440-million-us-by-2025-2019-10-23>, 2019) where an exhaustive

study targeting current market trends influencing the business across assorted regions, there is a research gap in the development of water generator and in particular using solar energy for remote areas. Significant details related to market size, market share, applications, and statistics are needed to be put together to provide the ensemble prediction of the ambient water production to the industry. The further research should focus on a comprehensive competitor's analysis and highlight the growth strategies for this technology.

This present study is intended to investigate and analyze the performance of solar water machine that produces potable water after a dehumidification process. The numerical model presented in this study was established after the conservation of mass and energy equations of the different control volumes of the solar power generator. The model was numerically solved under different conditions such as solar radiation, air humidity, air temperature and different air stream flows. Finally, the published data were compared to the model predicted results for validation purposes.

## 2. MATHEMATICAL MODEL

The proposed water generating hybrid system extracts water from water vapor availed at the ambient by means of condensation of the water vapor into water and with ozone generator and filters potable water can be produced. This process occurs by cooling down the air below its dew point using vapor compression system known as a dehumidifier to generate water potable. This hybrid system is composed of a dehumidifier and driven by power supplied by solar PV panels [Figure 1](#). Therefore, this solar water generating system is fully independent from the grid and can be implemented and used in remote areas.

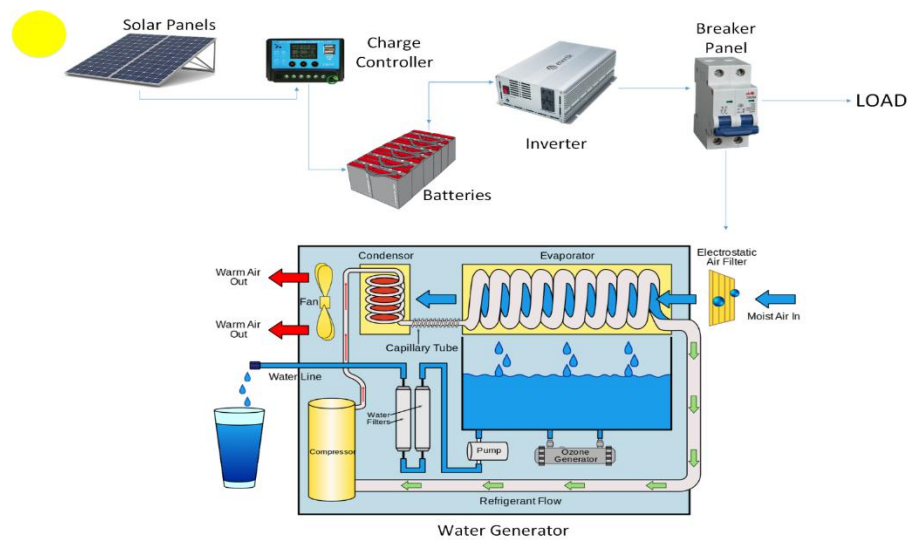


Figure-1. Concept of solar water hybrid generator.

The rate of water produced has a function dependence on the atmospheric conditions; temperature, humidity, the volume of air passing over the condensing coil, and the vapor compression compressor thermal capacity to cool down the evaporator coil. The proposed system has zero carbon footprints compared to others such as reverse osmosis seawater desalination and desiccants (Bagheri, 2018; Bergmair et al., 2014; Beysens et al., 2003).

From the laws of thermodynamic, the required air flow to remove an amount of moisture in a specific space can be calculated as [Ekad et al. \(2018\); VanWylen and Sonntag \(1985\);](#)

$$L = G / (x_r - x_m) \tag{1}$$

where

L: air flow (kg/h)

G: moisture in the space (kg/h)

$x_r$ : humidity ratio of air (kgH<sub>2</sub>O/kg dry air)

$x_m$ : humidity ratio in make-up air (kgH<sub>2</sub>O/kg dry air)

Whereas, humidity ratio  $x_r$  is expressed by [Firmanda et al. \(2011\)](#);

$$x_r = m_w / m_a \quad (2)$$

where

$x_r$ : humidity ratio (kg<sub>water</sub>/kg<sub>dry air</sub>, lb<sub>water</sub>/lb<sub>dry air</sub>)

$m_w$ : mass of water vapor (kg, lb)

$m_a$ : mass of dry air (kg, lb)

The ideal gas implies that the humidity ratio can be determined as follows [Firmanda et al. \(2011\)](#);

$$x = 0.62198 p_w / (p_a - p_w) \quad (3)$$

where

$p_w$ : partial pressure of water vapor in moist air (Pa, psi)

$p_a$ : atmospheric pressure of moist air (Pa, psi)

The maximum amount of water vapor in the air can be condensed at  $p_w = p_{ws}$  the saturation pressure of water vapor, therefore, [Equation 3](#) can be rewritten as [Firmanda et al. \(2011\)](#);

$$x_s = 0.62198 p_{ws} / (p_a - p_{ws}) \quad (4)$$

where

$X_s$  and  $P_{ws}$  represent the maximum saturation humidity ratio of air (kg<sub>water</sub>/kg<sub>air</sub>, lb<sub>water</sub>/lb<sub>dry air</sub>) and saturation pressure of water, respectively

References ([Abdullahi et al., 2017](#)) <https://physics.stackexchange.com/2019>, 2019 reported that there is strong dependency between the solar radiation and humidity, and the relative humidity has effects on solar radiation in a particular location. Also, the higher the solar radiation results in lower relative humidity. Since the present concept depends upon the solar radiation to drive the process, it was felt that the relative humidity must be taken into considerations. The relative humidity is defined as the ratio of vapor partial pressure in the air to the saturation vapor partial pressure if the air at the actual dry bulb temperature and can be given by [Firmanda et al. \(2011\)](#); Relative humidity as the ratio of vapor partial pressure in the air - to the saturation vapor partial pressure if the air at the actual dry bulb temperature. [Figures 3](#) and [4](#) show the profiles of the solar radiation and the relative humidity during the day at different months. The data presented in figures are in full agreement with findings of references ([Abdullahi et al., 2017](#)) (<https://physics.stackexchange.com/2019>, 2019). Furthermore, the strong dependency between the solar radiation and humidity ratio, and the relative humidity have significant impact on the amount of water vapor to be condensed, which the core of this study. Therefore, [Figure 5](#) was constructed to establish this dependency relationship used in the following section.

$$\phi = p_w / p_{ws} \text{ 100\%} \quad (5)$$

where;  $\phi$  and  $p_w$  represent the relative humidity [%] and the vapor partial pressure [bar], respectively.

### 2.1. Dehumidifier Model

The dehumidifier thermodynamic cycle is shown in [Figure 2](#) where the refrigerant vapor is compressed to high pressure and temperature conditions and enters into the condenser where sensible and latent heat are dissipated to the ambient. This is followed by throttling process through the expansion device that lead to the evaporator where the air water vapor is condensed to generate the water. Then the refrigerant is recycled to the compressor where the thermodynamic cycle continues. The following presents the steady state energy balance equations of the dehumidifier shown in [Figure 1](#) where we have four essential components and control; compressor, condenser, expansion device and evaporator where the condensation of the humidity or water vapor occurs.

A Quaternary components refrigerant mixture composed of refrigerants; R134a, R125, R 152a and R236fa was used in the dehumidifier loop to maximize potable water generation. Thermodynamic and thermophysical properties of the mixture in question (C.F. Figure 7) were determined after REFPROP program (NIST, 2013).

The compressor power required to drive the dehumidifier is:

$$Q_{comp} = \eta_c * m_{ref} * (h_2 - h_1) \tag{6}$$

where  $\eta_c$  and  $m_{ref}$  are the compressor efficiency and the refrigerant mass flow rate, respectively.  $h_2$  and  $h_1$  represent the enthalpies at the entrance and exit of the compressor.

The condenser thermal heat capacity is calculated by the following equation:

$$Q_{cond} = \eta_{hx} * m_{ref} * (h_2 - h_3) \tag{7}$$

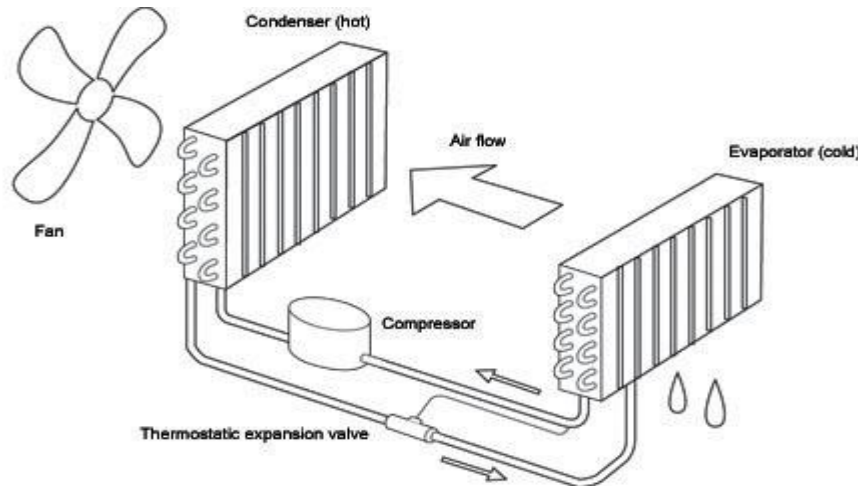


Figure-2. Dehumidifier thermodynamic cycle <https://physics.stackexchange.com/2019> (n.d).

Where,  $\eta_{hx}$ ,  $h_2$  and  $h_3$  represent the heat exchanger efficiency, enthalpies at the entrance and exit of the condenser, respectively.

$$h_3 = h_4 \tag{8}$$

where  $h_3$  and  $h_4$  are the enthalpies of the refrigerant at the inlet and outlet of the expansion throttling device. The enthalpies are determined using the thermodynamic property diagram of the refrigerant and pressure and temperature (Firmanda et al., 2011). The mass flow rate of refrigerant mixture is determined from the heat balance across the evaporator using Equations 1, 2 and 7.

Finally, the coefficient of performance COP which describes the dehumidifier is:

$$COP = Q_{evaporator} / Q_{comp} \tag{9}$$

$Q_{evaporator}$  and  $Q_{comp}$  are the thermal energy at the evaporator and compressor, respectively.

### 2.2. PV Solar Model

The solar photovoltaic panel is composed of various modules and each module is consisted of arrays and cells. The dynamic current output is obtained as follows as reported by Sami and Campoverde (2018) and Fahmy et al. (2010);

$$I_p = I_L - I_o \left[ \exp \left( \frac{q(V + I_p R_s)}{A k T_c} - \frac{V + I_p R_s}{R_{sh}} \right) \right] \tag{10}$$

$I_p$ : Output current of the PV module.

$I_L$  : Light generated current per module.

$I_o$  : Reverse saturation current per module.

$V$  : Terminal voltage per module.

$R_s$  : Diode series resistance per module.

$R_{sh}$  : Diode shunt resistance per module.

$q$ : Electric charge.

$k$  : The Boltzman constant.

$A$  : Diode ideality factor for the module.

The PV cell temperature,  $T_c$ , is significantly influenced by various factors such as solar radiations, ambient conditions, and wind speed as well as humidity. It is well known that the cell temperature impacts the PV output current, and performance, and its time-variation can be determined from references (Fahmy et al., 2010; Sami & Campoverde, 2018). The AC power of the inverter output  $P(t)$  as per Figure 1 is calculated using the inverter efficiency  $\eta_{inv}$ , output voltage between phases, neutral  $V_{fn}$ , and for single-phase current,  $I_o$  and the power factor,  $\cos\phi$  as follows;

$$PV(t) = \sqrt{3}\eta_{inv}V_{fn}I_o\cos\phi \tag{11}$$

And; the compressor is supplied by the PV solar panels as;

$$Q_{comp} = \sqrt{3} V I \cos\phi \tag{12}$$

The power supplied by the inverter defined by Equation 11 will drive the dehumidifier's compressor.

The power supplied by the PV panels can determine as follows;

$$Q_{comp} = P(t) = A_{PV} \alpha G_s \tag{13}$$

Where,  $A_{PV}$ ,  $\alpha$ , and  $G_s$  represent the PV solar panels area, Solar panel absorption efficiency and solar radiation, respectively.

The rating of the solar water hybrid generator is defined by the rate of water produced divided by the solar radiation to drive the dehumidifier and is determined by Equations 9 and 11 as follows;

$$Rating_{sc} = G / G_s \tag{14}$$

where;  $G_s$  represents the solar radiation in  $w/m^2$  and  $G$  is the moisture produced (kg/hr) and defined by equation (1), and units are kg/hr per  $w/m^2$

$$Efficiency_{ns} = G / (G_s + PV(t)) \tag{15}$$

where;  $G_s$  represents the solar radiation in  $w/m^2$  and  $G$  is the moisture produced (kg/hr) and defined in equation (1).  $PV(t)$  is defined by Equation 11.

### 2.3. Numerical Procedure

The numerical model established to determine the water production rate using the solar energy is described by mass and energy and refrigerant thermodynamic and thermophysical properties in Equations 1 through (15). The logical diagram presented in Figure 6 describes the several steps and calculations used to solve equations of the model in question. The logical diagram starts by inputting the ambient conditions, pressure, temperature and entropy of the refrigerant conditions circulating in the dehumidifier cycle, PV absorption efficiency and solar radiations. Then, equations were solved using an iteration technique. The iterations were performed using MATLAB iteration techniques until a converged solution is reached with acceptable iteration error as 0.05. To this end, the amount of the water vapor (kg/hr) in the air condenser and the PV solar panel area are calculated at each

ambient temperature as well as the other conditions. Next, the corresponding dehumidifier refrigeration cycle characteristics were determined. The calculations were repeated at different amount of water condensation; 1 through 5 kg/hr. Finally, at each condition, the Coefficient of Performance, COP of the dehumidifier, the hybrid system efficiency characteristic and moisture production rate per solar radiation ( $w/m^2$ ) are determined.

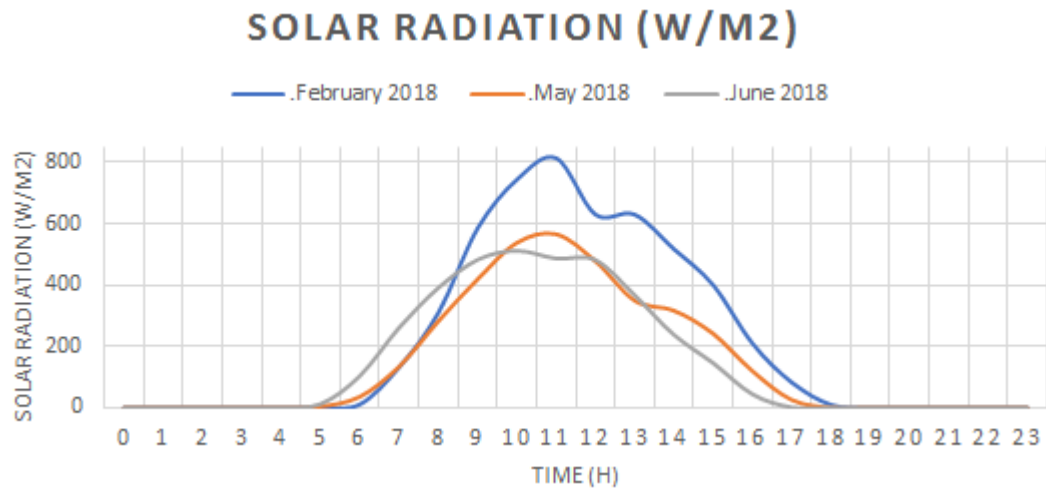


Figure-3. Solar radiation profile during the day.

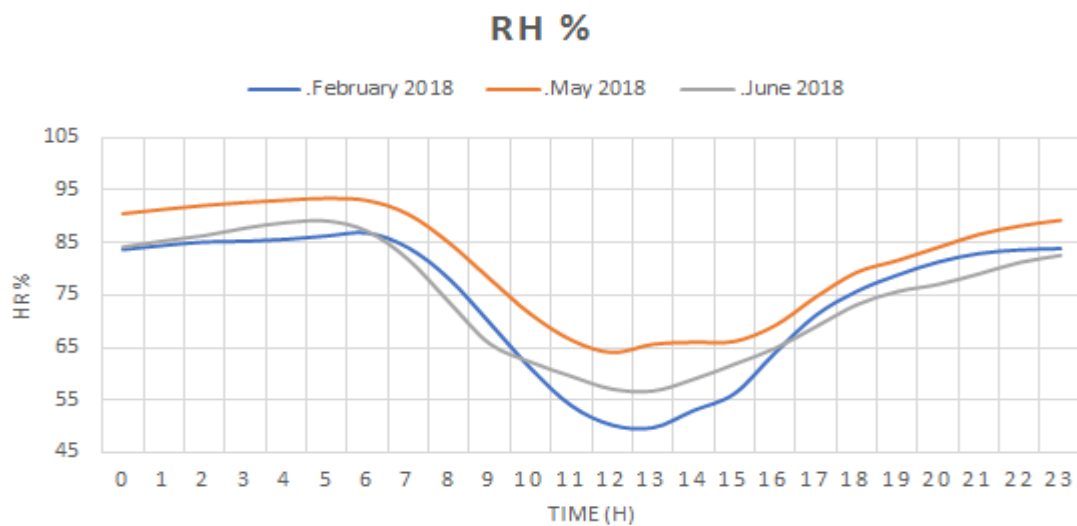


Figure-4. Relative humidity profile.

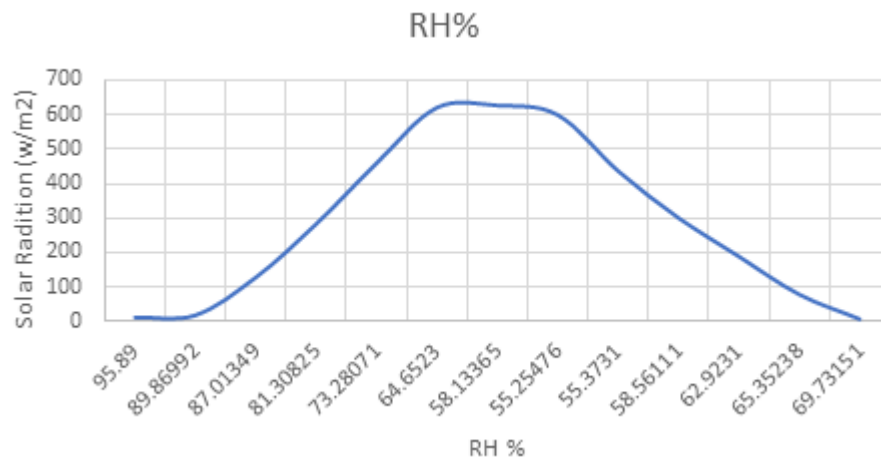


Figure-5. Relative humidity profile at different solar PV power.

### 3. RESULTS AND DISCUSSIONS

The parameters considered in this study are solar radiation, ambient temperature, relative humidity, speed and direction of the wind. However, it was noticed that the most influential parameters on the performance of the dehumidifier are the solar radiation, ambient temperature, and relative humidity. It was observed from data presented in the figures that high temperature is most frequently registered after noon, while the low temperature occurs mostly in the early morning hours. It should be noted that there is no significant relationship between temperature and relative humidity since, as discussed above, the maximum amount of water vapor in the air depends on the temperature, thus, the amount of water is not guaranteed to be the same at each temperature points. Moreover, as observed the humidity does not follow the temperature pattern nor vice versa, since each parameter is independent of the other. Therefore, our analysis intended to focus these parameters. The compressor power is significantly impacted by the air flow conditions such as the relative humidity and the ambient temperature. The different temperatures considered in this study are from 20°C through 45°C and relative humidity are between 35% and 97%. The study showed that radiation and energy captured per square meter was considerable, with a maximum radiation value 800 W/m<sup>2</sup> and a minimum value of 200.00 W/m<sup>2</sup> per day.

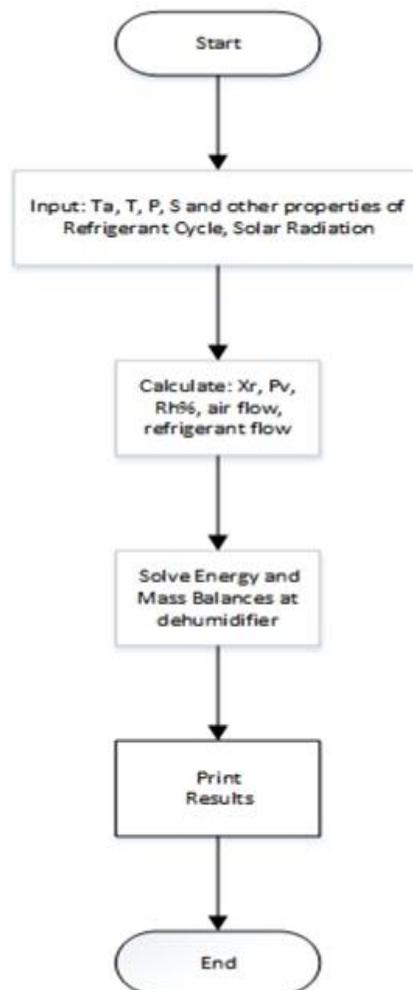


Figure-6. Logical diagram for numerical solution of the model.

It was assumed that the air temperature difference across the condenser is 20°C. The iteration procedure described Figure 6 lead to PV panel area of 1.617 m<sup>2</sup>. The cooling system compressor in this study was powered by a photovoltaic energy system consisting of several solar photovoltaic (PV) panels as per Figure 1 taking better advantage of the solar energy available, such as solar radiation. The dimensioning of the photovoltaic systems for

the proposed cooling capacities was carried out based upon the solar radiation. The compressor power was calculated under these conditions and the results were depicted in Figure 7 through Figure 10 where the compressor power plotted against the solar radiation and the other parameters. It is quite evident from the results presented in Figure 8 that the compressor power consumption is significantly dependent upon by profiles of the solar radiation and the relative humidity as demonstrated in Figure 5. It should be noted that moist air is a non-reactive mixture of dry air and water vapor. The mass ratio of water vapor and dry air is known as specific humidity, its variation is fully depending on the area's ambient conditions. It is quite known that in a given thermodynamic state, each of the components has certain properties that help determine the amount of energy required to condense water vapor. This can be noticed from the results displayed in these two figures that the higher the relative humidity the lower the solar radiation. In addition, as can be demonstrated easily by Equation 5 that higher relative humidity results in higher amount of water condensed per unit time. During the dehumidification process, mass and energy exchanges took place. As per the above equations, energy exchanges were estimated by considering the properties of the mixture under the system's inlet and outlet ambient conditions. Inlet properties were determined by the system surroundings, while the outlet parameters were determined by the properties required for condensation to take place.

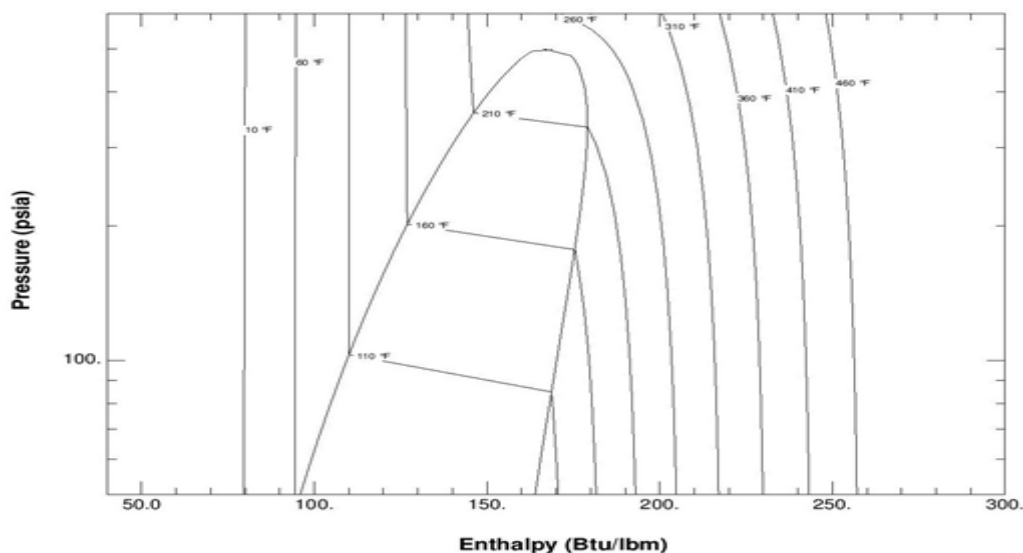


Figure-7. Pressure Enthalpy diagram for the refrigerant used in the dehumidifier.

In the following sections, the most influential ambient parameters on the amount of water condensation per unit time are the ambient temperature and the solar radiation. Therefore, Figures 10 through Figure 12 have been constructed to analyze the impact of these parameters. In particular, Figure 10 shows the impact of the ambient temperature and the dehumidifier air flow on the rate of water produced. At constant ambient temperature the higher the air flow at the evaporator the higher the water rate produced. Also, the displayed results in this figure illustrate that at a constant water production rate the higher the ambient temperature the lower the air flow.

Figure 11 has been constructed to study the effects of the ambient temperature and the rate of water production on the evaporator thermal capacity. The results displayed in this figure demonstrate that in general higher ambient temperatures reduces the evaporator capacity of the dehumidifier and at constant ambient temperature the higher the rate of water production the higher the evaporator thermal capacity. This was obviously expected. Figures 10 and .11 are closely interrelated since higher evaporator air flow results in higher evaporator thermal capacity. This is clearly demonstrated by Equations 1 through (4).

As per Equations 1 the air flow, humidity ratio and the evaporator thermal capacity are interrelated, therefore, the compressor power is significantly influenced by the ambient temperature, solar radiation and the rate of water

production. Thus, Figure 11 was constructed to illustrate this interrelationship between the different parameters involved in the process of water production using solar energy as source of energy.

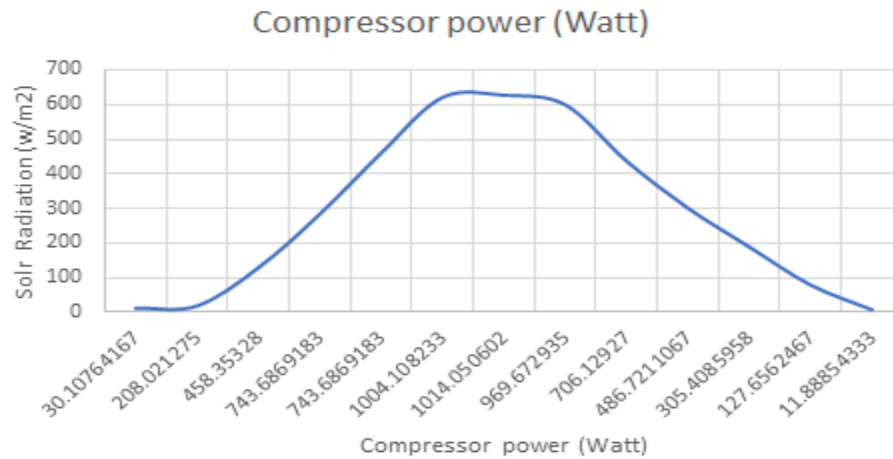


Figure-8. Compressor Power at different relative humidity.

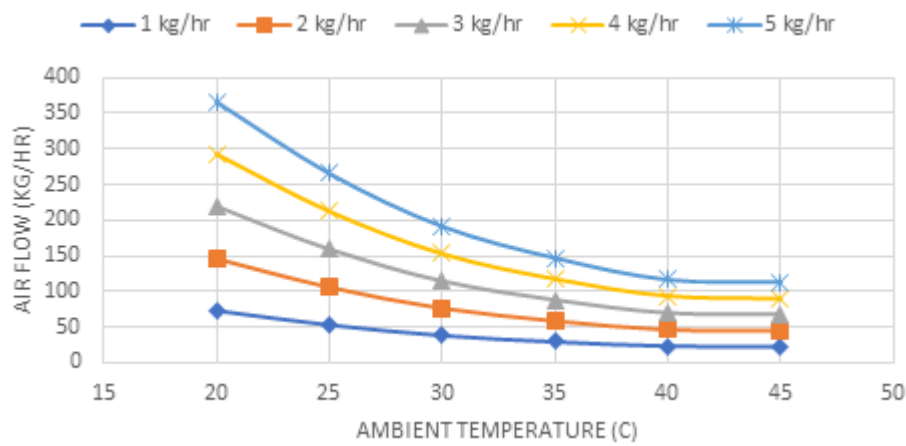


Figure-9. Dehumidifier air flow rate Compressor at different water condensation (kg/hr).

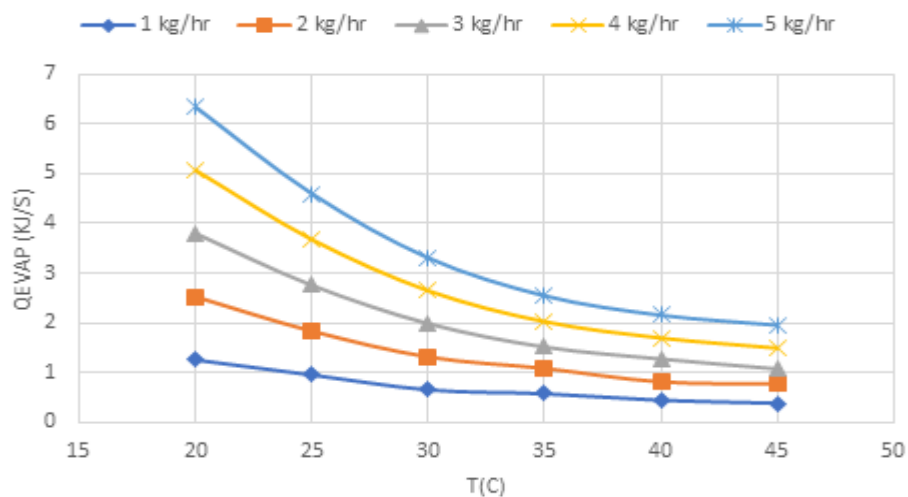


Figure-10. Evaporator capacity at different ambient temperatures.

Theoretically, it's expected that the water vapor in the incoming mixture to be completely condensed, but in practice, the water vapor does not completely condense. Therefore, in case of incoming dry air, it only undergoes a temperature change, being the means of transport for water vapor, and can be neglected.

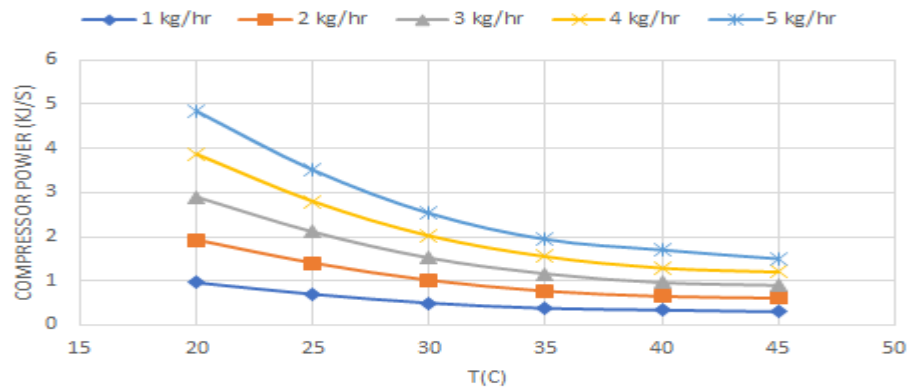


Figure-11. Compressor Power at different ambient temperatures.

Further to results displayed in Figure 5 and Figure 9 as well as Figure 12 it can be easily shown that the higher the relative humidity, the higher the rate of water production and lower the ambient temperature and the higher the compressor power, which is a consequence of higher evaporator thermal capacity.

As discussed earlier in this paper, the humidity ratio influences the rate of amount of water condensed across the evaporator and that in turn, impacts the compressor power. Therefore, it felt that it is worthwhile, constructing the Figure 12 at different rates of condensed water to demonstrate that influence. The results depicted in this figure clearly illustrate that higher humidity ratios reduce the compressor power consumed by the dehumidifier and also can be seen that at constant humidity ratio the higher the rate of water production the higher compressor power consumed. Therefore, the humidity ratio plays a significant role in determining the compressor power and the rate of water produced.

The characteristics of the humidifier hybrid driven by solar radiation can be expressed by and has functional dependence on the ratio of the rate of water produced, air flow, evaporator thermal capacity and compressor power which are determined by Equations 1 through (15). Figure 13 has been established to demonstrate the functional dependence of the evaporator air flow on the ambient temperature efficiency of the dehumidifier hybrid system. It is evident from the data depicted in this figure that the lower the ambient temperature the higher the air flow rate. This signifies that the higher the air flow the higher the power consumed. This is credited to that higher temperatures are associated with lower humidity ratio and in turn reduce the air densities and consequently the compressor power. This is quite evident from Figure 14 where the evaporator thermal capacity was depicted against the humidity ratio. The figure demonstrates that the lower the humidity ratio the higher the evaporator thermal capacity. Also, it shows that the higher the rate of water production the higher the evaporator thermal capacity as well as higher water production is associated with higher air flow and compressor power consumption.

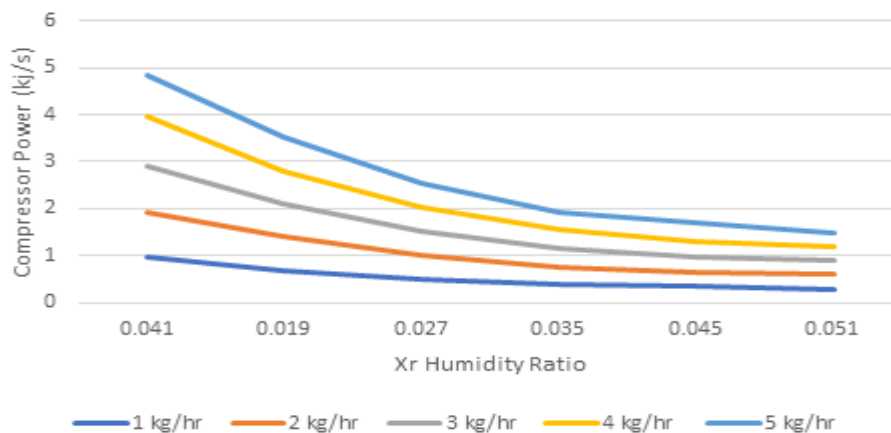


Figure-12. Compressor power versus humidity ratio at different water rate production.

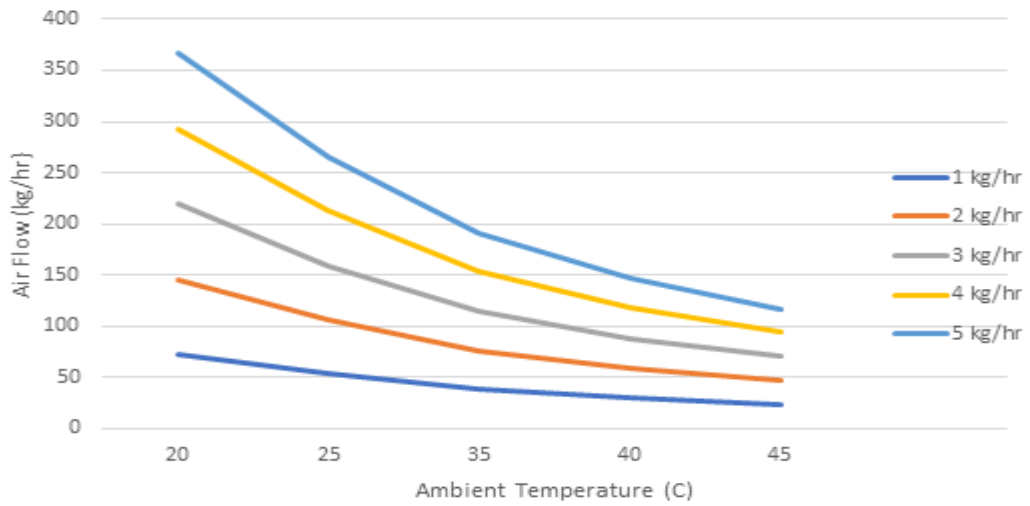


Figure-13. Evaporator air flow versus ambient temperature at different water rate production.

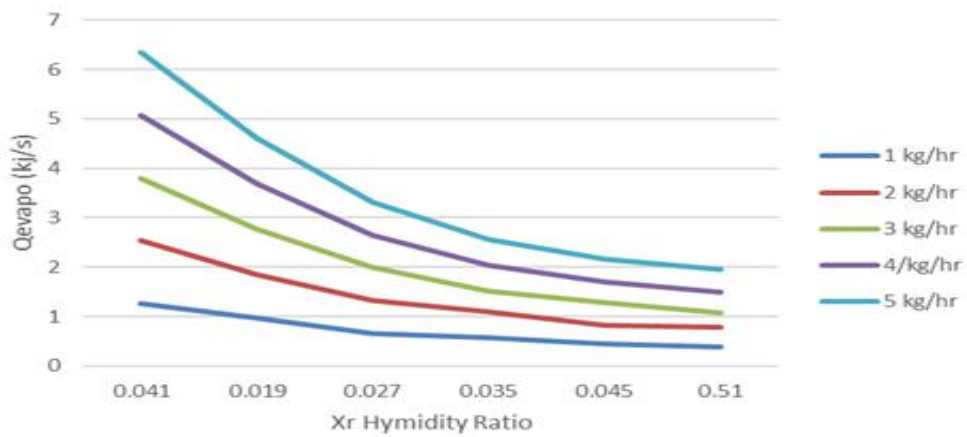


Figure-14. Evaporator thermal capacity versus humidity ratio ambient at different water rate production.

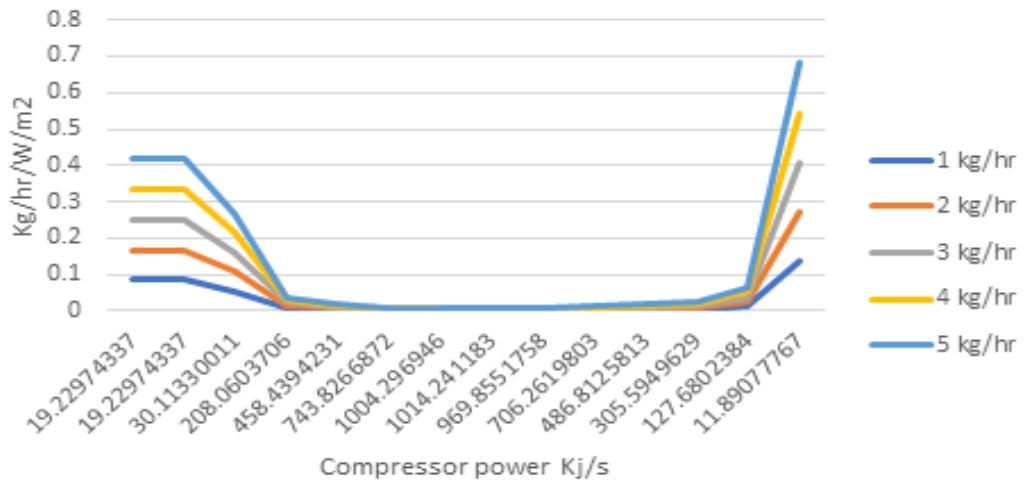


Figure-15. Hybrid system efficiency at different compressor power.

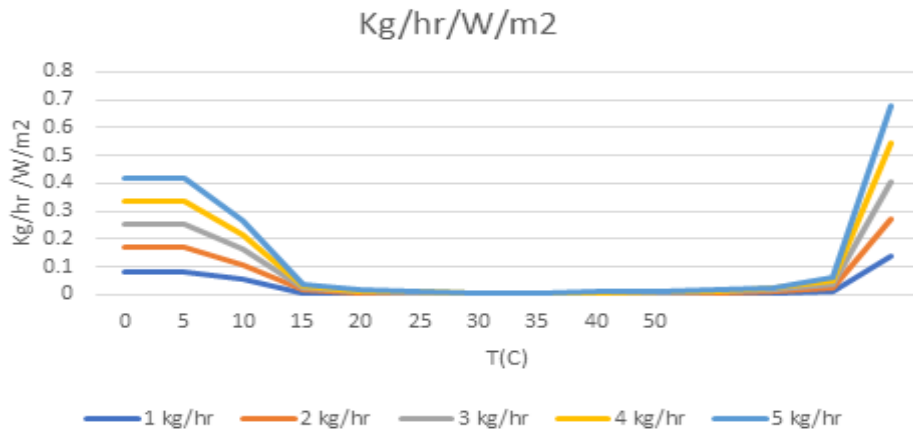


Figure-16. Rating of water production per Solar radiation at different ambient temperatures.

The rating of the solar water dehumidifier hybrid generator is defined by the rate of water produced divided by the solar radiation to drive the dehumidifier and is determined by Equations 9, 11 and 14. Figures 15 and 16 have been constructed to analyze the dehumidifier ratings where the rating in kg/hr/W/m<sup>2</sup> is plotted against the compressor power and the ambient temperature, respectively. It is evident from Figures 15 that the ratings follow the solar radiations profile, and the ratings obviously is higher at higher water production rate at lower solar radiation. Furthermore, the ratings follow the solar radiation and the ambient temperature profile as demonstrated in Figure 16.

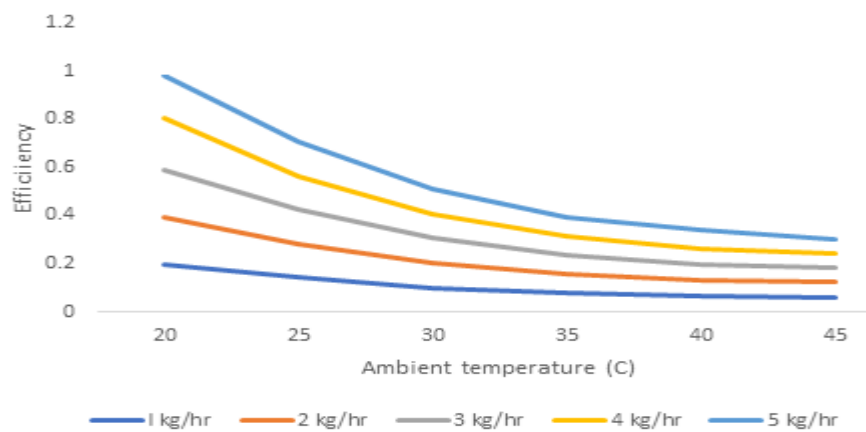


Figure-17. Hybrid system efficiency at different ambient temperatures.

Figure 17 was constructed to illustrate the functional dependence of the hybrid system efficiency on the key parameters of the system, ambient temperature, water rate of production, relative humidity and solar radiations. The efficiency is calculated by Equation 15 and Equation 11 as well as Equation 1. The results displayed in this figure demonstrate that the lower the ambient temperature the higher the hybrid system efficiency and also the hybrid system efficiency increases at lower ambient temperature and higher water production rate.

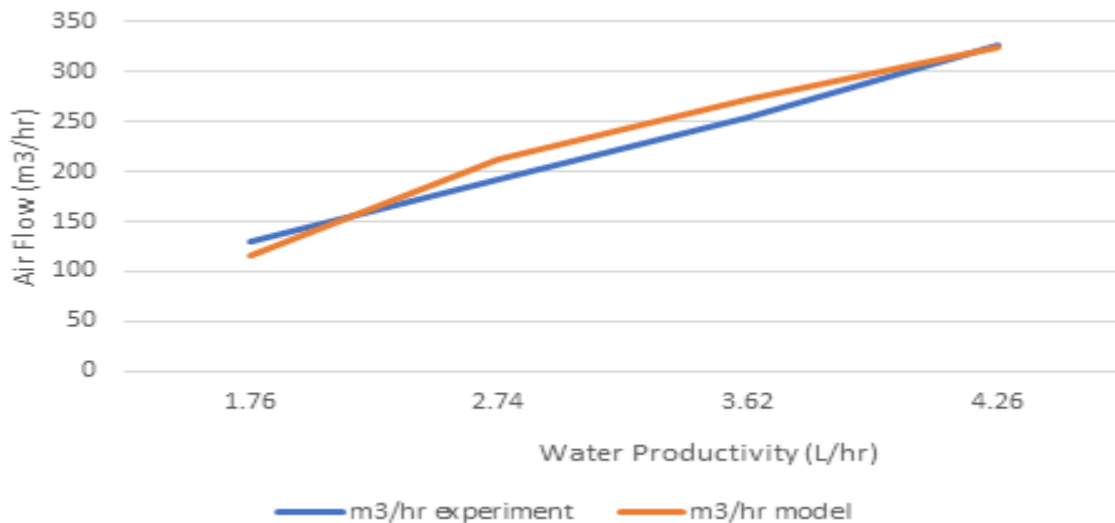


Figure-18. Comparison between model and experiment reference (Suryaningsih & Nurhilal, 2016) at ambient temperatures.

For the purpose of the validation of the model developed after Equation 1 through (15), Figure 18 has been constructed where the dehumidifier air flow was plotted against the water productivity using the PV solar panel. The experimental data were extracted from reference (Suryaningsih & Nurhilal, 2016) where an atmospheric water generator (AWG) was used for freshwater recovery directly from the moisture content of water vapor from the air. It appears from the results depicted in Figure 18 that the model and experimental data obtained after reference (Suryaningsih & Nurhilal, 2016) are in fair agreement. However, some discrepancies exist between the model prediction and experimental data. This could be ascribed to the different assumptions and relationships used in the model to calculate the water productivity. On the average the discrepancies were around 7.5%.

Finally, since this water generation of clean water is intended for remote areas without power, in great need of clean water, we believe that other energy sources can be used directly in the processes to drive the cooling system compressor. Such systems can include geothermal energy or solar energy, or indirect means that produce electrical energy by means of wind energy or photovoltaic solar-PV-Thermal hybrid system that provide the water generator with electrical energy needed for its operation.

#### 4. CONCLUSIONS

The objective of this study is to investigate and analyze the performance of solar water machine that produces potable water after a dehumidification process. The numerical model presented in this study was established after the conservation of the mass and energy equations of the different control volumes of the system. The model was numerically solved under different conditions such as solar radiation, air humidity, air temperature and different air stream flows.

Obviously, the ratings of the dehumidifier are higher at higher water production rate at lower solar radiation. Also, the results show that the lower the humidity ratio the higher the evaporator thermal capacity. Also, it shows that the higher the rate of water production the higher the evaporator thermal capacity as well as higher water production is associated with higher air flow and compressor power consumption. In addition, it can be concluded that the lower the ambient temperature the higher the hybrid system efficiency and also the hybrid system efficiency increases at lower ambient temperature and higher water production rate.

The model predictions compared fairly with the data available in the literature and the discrepancies were with 7.5 %.

**Funding:** This study received no specific financial support.

**Competing Interests:** The author declares that there are no conflicts of interests regarding the publication of this paper.

**Acknowledgement:** The research work presented in this paper was made possible through the support of the Catholic University of Cuenca. The author greatly appreciates the efforts of Edwin Marin in the lengthy calculations using finite difference formulation and experimental work.

## REFERENCES

- Abdullahi, S., Ayegba, M. A., & Adejoh, J. (2017). Impacts of relative humidity and mean air temperature on global solar radiations of Ikeja, Lagos, Nigeria. *International Journal of Scientific and Research Publications*, 7(2), 315-319.
- Bagheri, F. (2018). Performance investigation of atmospheric water harvesting systems. *Water Resources and Industry*, 20, 23-28. Available at: <https://doi.org/10.1016/j.wri.2018.08.001>.
- Bergmair, D., Metz, S. J., De Lange, H., & Van Steenhoven, A. (2014). System analysis of membrane facilitated water generation from air humidity. *Desalination*, 339(1), 26-33.
- Beysens, D., Milimouk, I., Nikolayev, V., Muselli, M., & Marcillat, J. (2003). Using radiative cooling to condense atmospheric vapor: A study to improve water yield. *Journal of Hydrology*, 276(1-4), 1-11. Available at: [https://doi.org/10.1016/S0022-1694\(03\)00025-8](https://doi.org/10.1016/S0022-1694(03)00025-8).
- Ekad, A., Pawar, T., Yeole, N., Taksale, A., & Gajjar, A. (2018). Solar powered atmospheric water generator and overview on AWG technologies. *International Journal of Innovative Research in Science, Engineering and Technology*, 7(1), 71-79.
- Fahmy, F. H., Nafeh, A. A., Ahamed, N. M., & Farghally, H. M. (2010). *A simulation model for predicting the performance of PV/Wind- powered geothermal space heating gystem in Egypt*. Paper presented at the In Proceedings of International Conference on Renewable Energies and Power Quality (ICREPQ'10), Granada, Spain, 23-25 March 2010; doi:10.24084/repqj08.734.
- Firmanda, A. R., D., Ihtsham, u. H. G. S., & Shiraz Aris, M. (2011). Hourly solar radiation estimation using ambient temperature and relative humidity data. *International Journal of Environmental Science and Development*, 2(3), 188-193.
- Habeebullah, B. A. (2009). Potential use of evaporator coils for water extraction in hot and humid areas. *Desalination*, 237(1-3), 330-345. Available at: <https://doi.org/10.1016/j.desal.2008.01.025>.
- Hellström, B. (1969). Potable water extracted from the air report on laboratory experiments. *Journal of Hydrology*, 9(1), 1-19. Available at: [https://doi.org/10.1016/0022-1694\(69\)90011-0](https://doi.org/10.1016/0022-1694(69)90011-0).
- <https://physics.stackexchange.com/2019>. (n.d).
- Julio, A., Mendoza-Escamilli, Francisco, J. H.-R., Pedro, C.-A., María, Z. S.-L., Josefa, M.-M., R. . . Francisco, J. M.-L. (2019). A feasibility study on the use of an atmospheric water generator (AWG) for the harvesting of fresh water in a Semi-Arid Region affected by Mining Pollution. *Applied Sciences*, 9(16), 3278. Available at: 10.3390/app9163278.
- Jury, W. A., & Vaux Jr, H. J. (2007). The emerging global water crisis: Managing scarcity and conflict between water users. *Advances in Agronomy*, 95(7), 1-76. Available at: [https://doi.org/10.1016/S0065-2113\(07\)95001-4](https://doi.org/10.1016/S0065-2113(07)95001-4).
- Kabeel, A., Abdulaziz, M., & El-Said, E. M. (2016). Solar-based atmospheric water generator utilisation of a fresh water recovery: A numerical study. *International Journal of Ambient Energy*, 37(1), 68-75.
- Liu, S., He, W., Hu, D., Lv, S., Chen, D., Wu, X., . . . Li, S. (2017). Experimental analysis of a portable atmospheric water generator by thermoelectric cooling method. *Energy Procedia*, 142, 1609-1614. Available at: <https://doi.org/10.1016/j.egypro.2017.12.538>.
- Mekonnen, M. M., & Hoekstra, A. Y. (2016). Four billion people facing severe water scarcity. *Science Advances*, 2(2), e1500323. Available at: <https://doi.org/10.1126/sciadv.1500323>.
- Milani, D., Qadir, A., Vassallo, A., Chiesa, M., & Abbas, A. (2014). Experimentally validated model for atmospheric water generation using a solar assisted desiccant dehumidification system. *Energy and Buildings*, 77, 236-246. Available at: <https://doi.org/10.1016/j.enbuild.2014.03.041>.
- Nikolayev, V. S., Beysens, D., Gioda, A., Miliouk, I., Katiushin, E., & Morel, J. P. (1996). Water recovery from dew. *Journal of Hydrology*, 1(182), 19-35.

NIST. (2013). Excel applications

Sami, S., & Campoverde, C. (2018). Dynamic simulation and modeling of a novel combined hybrid photovoltaic-thermal panel hybrid system. *International Journal of Sustainable Energy and Environmental Research*, 7(1), 1-23. Available at: <https://doi.org/10.18488/journal.13.2017.71.1.23>.

Scrivani, A., & Bardi, U. (2008). A study of the use of solar concentrating plants for the atmospheric water vapour extraction from ambient air in the Middle East and Northern Africa region. *Desalination*, 220(1-3), 592-599. Available at: <https://doi.org/10.1016/j.desal.2007.04.060>.

Sharan, G., Beysens, D., & Milimouk-Melnitchouk, I. (2007). A study of dew water yields on Galvanized iron roofs in Kothara (North-West India). *Journal of Arid Environments*, 69(2), 259-269. Available at: <https://doi.org/10.1016/j.jaridenv.2006.09.004>.

Suryaningsih, S., & Nurhilal, O. (2016). *Optimal design of an atmospheric water generator (AWG) based on thermo-electric cooler (TEC) for drought in rural area*. Paper presented at the AIP Conference Proceedings 1712, 030009.

VanWylen, G. J., & Sonntag, R. E. (1985). *Fundamentals of classical thermodynamics* (3rd ed.). John Willey, & Sons.

*Views and opinions expressed in this article are the views and opinions of the author(s), International Journal of Sustainable Energy and Environmental Research shall not be responsible or answerable for any loss, damage or liability etc. caused in relation to/arising out of the use of the content.*